Design and Simulation of Planar Antennas using MATLAB Antenna Toolbox

Dimitrios Karatis 10775, *Electrical and Computer Engineering, AUTH*

***Abstract*—This project focuses on the design and simulation of planar antennas using the Antenna Toolbox in MATLAB. Following the selection of a scientific article, the structure and properties of a specific antenna are recreated through MATLAB scripting. The key outputs include the reflection coefficient, radiation patterns, and other electromagnetic characteristics. The goal is to validate and replicate the article's findings through simulation and analysis.**

***Index Terms*—Antenna Toolbox, MATLAB, planar antennas, reflection coefficient, radiation pattern, electromagnetic simulation.**

I. Introduction

This work aims to design and simulate planar antennas with the help of MATLAB's Antenna Toolbox. The design is based on a scientific article selected according to the student's surname. The project includes analysis of antenna geometry, performance evaluation, and comparison with the published results.

Article Selection

The paper selected for this project is titled ***"Compact H-Ring Antenna with Dual-Band Operation for Wireless Sensors and RFID Tag Systems in ISM Frequency Bands"*** by Nasser Ojaroudi and Mohammad Ojaroudi.

A. Design Process in MATLAB

The antenna geometry was modeled using MATLAB's built-in primitives and custom scripts. The following steps were followed:

- Creation of geometry using `antenna.Rectangle` and Boolean operations.
- Definition of substrate, ground plane, and feeding mechanism.
- Use of `pattern` as well as other functions to compute reflection coefficient S_{11}, Smith diagrams etc.

Antenna Design Methodology

The antenna design process was carried out in three sequential stages, resulting in three distinct antenna configurations—Antenna 1, Antenna 2, and the final proposed Antenna 3. Each stage introduced specific structural modifications aimed at improving the impedance matching, bandwidth, and dual-band performance necessary for modern wireless applications.

This document was prepared by Dimitrios Karatis as part of the first assignment for the Advanced Antennas course at Aristotle University of Thessaloniki.

Antenna 1 was designed as the baseline structure, comprising a simple rectangular monopole fed by a microstrip line and printed on an FR4 substrate with a partial ground plane. This initial structure was tuned to resonate around a single frequency near 3 to 5 GHz. However, it exhibited limited bandwidth at 5 to 6 GHz as shown in Figure 8.

The design, illustrated in Figure 1, consists of a rectangular radiating patch with dimensions $L_{\text{patch}} = 10\,\text{mm}$ and $W_{\text{patch}} = 10\,\text{mm}$ ($W_{h1} + 2 \times W_{h2}$), fed by a microstrip transmission line of width $W_f = 1.5\,\text{mm}$ and length $L_f = 7\,\text{mm}$. The ground plane, measuring $12\,\text{mm} \times 4\,\text{mm}$, is positioned on the opposite side of the $0.8\,\text{mm}$ thick substrate. The antenna structure was modeled using MATLAB's Antenna Toolbox, where the patch, feed line, and ground plane were defined as perfect electric conductor (PEC) rectangles with carefully calculated center positions. The feed point was located at $(x_{\text{mid}}, L_{gnd})$. For accurate simulation results, the mesh was refined with maximum edge length of 0.01λ and minimum edge length of 0.001λ, using a growth rate of 0.7 to balance computational efficiency and numerical precision.

Antenna 2 incorporates a notable design modification by etching an H-shaped slot into the radiating patch of Antenna 1. This alteration shifted the fundamental resonant mode of the antenna to the frequency range of approximately 4 to 4.8 GHz, quiet different from the results of the paper.

The second antenna design, shown in Figure 2, features an H-shaped monopole structure fabricated on the same FR4 substrate ($\epsilon_r = 4.4$, $\tan\delta = 0.018$) with thickness $0.8\,\text{mm}$. The H-shaped radiating element consists of three rectangular components: two vertical arms (each $2\,\text{mm} \times 10\,\text{mm}$) and a central horizontal connector ($6\,\text{mm} \times 2\,\text{mm}$), carefully positioned at coordinates $\left(x_{\text{mid}} \pm (\frac{W_h}{2} + \frac{W_{h3}}{2})\,\text{mm},\ y_{\text{patch}}\right)$ and $(x_{\text{mid}}, y_{\text{patch}})$ respectively. The structure is fed by a $1.5\,\text{mm}$ wide microstrip line of length $11\,\text{mm}$ ($L_f + L_{\text{gnd}}$). The ground plane dimensions ($12\,\text{mm} \times 4\,\text{mm}$) and substrate size ($12\,\text{mm} \times 18\,\text{mm}$) match the first design for consistent comparison. The H-shaped configuration was implemented by combining three separate perfect electric conductor (PEC) rectangles using Boolean addition operations. Simulation parameters identical to the first antenna were maintained, with S-parameters analyzed across the $1.5\,\text{GHz}$ to $6.5\,\text{GHz}$ range to evaluate the performance characteristics of this topology.

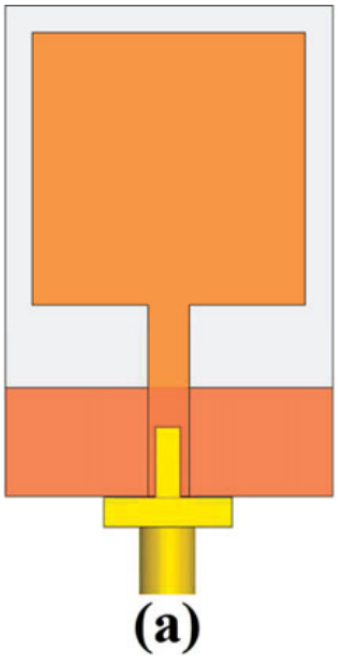

Fig. 1: The first antenna

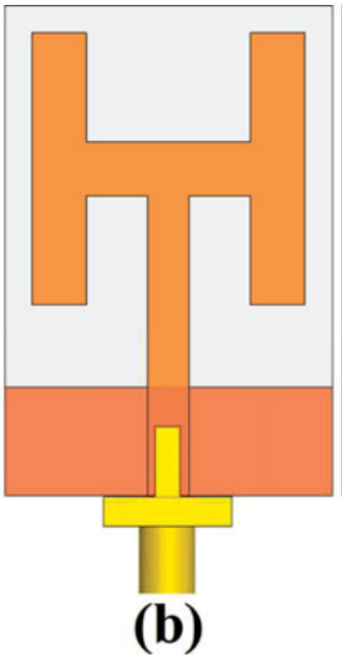

Fig. 2: The second antenna

Antenna 3, the final proposed design, added dual-band behavior by incorporating an H-shaped ring structure and additional slots on the main patch. These enhancements were introduced to improve current distribution and surface wave suppression, which in turn broadened the bandwidth by adding a new frequency band. The H-ring geometry also helped to miniaturize the antenna footprint while maintaining efficient radiation characteristics. This antenna demonstrated better S-parameter results than the previous one, with reflection coefficients almost at -10 dB in both 3–4.1 GHz and 5.1–6.1 GHz ranges.

The optimized third antenna design, depicted in Figures 3 and 4, represents an advanced evolution of the H-shaped monopole with additional parasitic elements for enhanced performance. This sophisticated structure maintains the same FR4 substrate properties ($\epsilon_r = 4.4$, $\tan\delta = 0.018$, thickness $0.8\,\text{mm}$) but incorporates twelve carefully positioned rectangular elements forming a complex radiating system. The design features two main vertical arms ($10\,\text{mm} \times 0.5\,\text{mm}$), complemented by four smaller vertical elements ($4\,\text{mm} \times 0.5\,\text{mm}$) and six horizontal connectors (four measuring $2\,\text{mm} \times 0.5\,\text{mm}$ and two central $6\,\text{mm} \times 0.5\,\text{mm}$ elements). The feed system consists of an $11\,\text{mm}$ long microstrip line ($1.5\,\text{mm}$ width), identical to previous designs for consistent comparison. The intricate geometry was constructed through Boolean addition of thirteen perfect electric conductor (PEC) rectangles (twelve radiating elements plus feed line), precisely positioned using calculated center coordinates. This enhanced topology, while maintaining the same $12\,\text{mm} \times 18\,\text{mm}$ board size and $12\,\text{mm} \times 4\,\text{mm}$ ground plane as previous iterations, demonstrates improved impedance matching across the $1.5\,\text{GHz}$ to $6.5\,\text{GHz}$ operational bandwidth in terms of the previous antenna, as evidenced by its S-parameter characteristics.

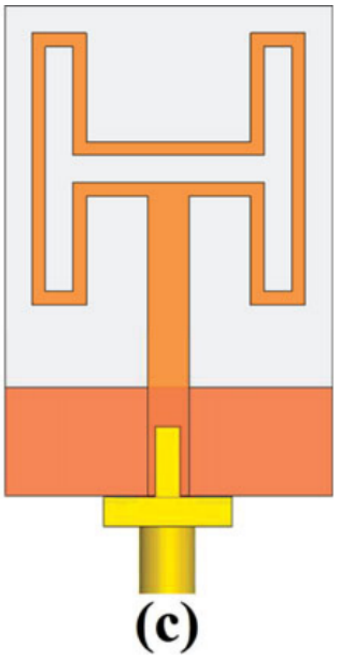

Fig. 3: The third antenna

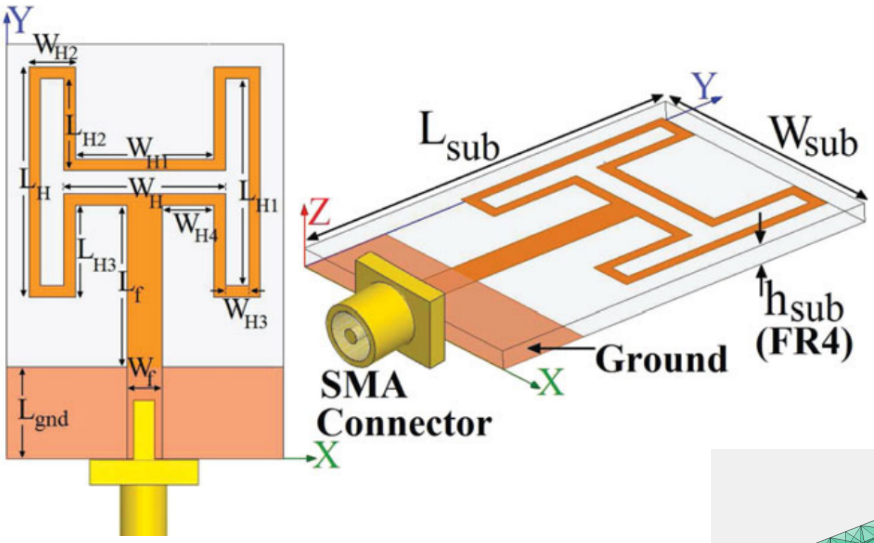

Fig. 4: The third antenna

Detailed calculations as well as code can be found in the antenna_designs.m file.

RESULTS

Below are the 3 antenna designs using MATLAB:

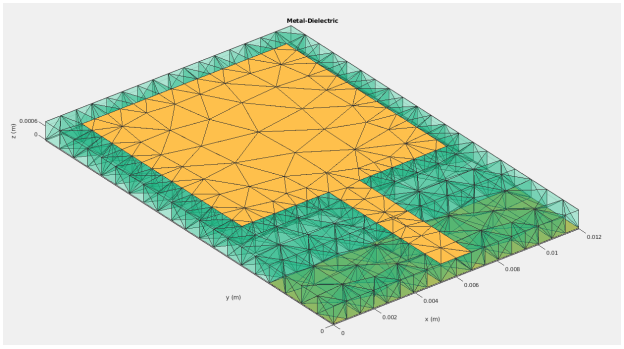

Fig. 5: First antenna design

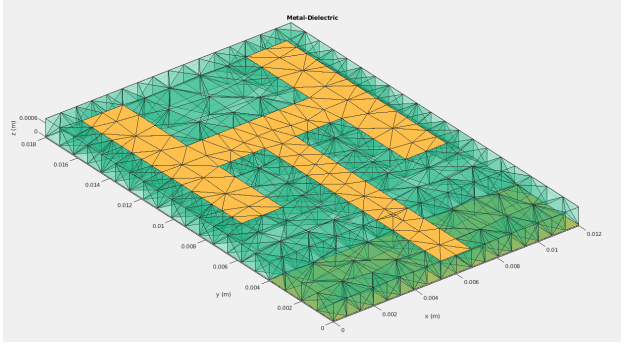

Fig. 6: Second antenna design

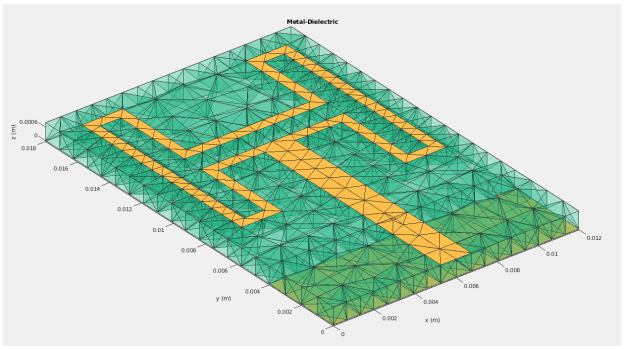

Fig. 7: Third antenna design

II. ANTENNA PERFORMANCE ANALYSIS

A. Impedance Matching and Bandwidth

Figure 8 presents a comparative analysis between the simulated S_{11} parameters of three antenna structures: the Basic Structure (Ordinary Square Monopole Antenna), the H-Shaped Monopole Antenna, and the Proposed Monopole Antenna. The results from the reference paper (Figure 9) demonstrate distinct dual-band behavior for the Proposed Monopole Antenna with strong resonances around 2.6 GHz and 5.8 GHz, both achieving return losses below -30 dB. In contrast, the reconstructed simulation results (Figure 8) also show a similar dual-resonance behavior for the Proposed Monopole Antenna, with notable notches at approximately the same frequencies and return losses nearing -10 dB or lower. The H-Shaped Monopole in both cases exhibits a single deep resonance near 5.5 GHz. Meanwhile, the Basic Structure remains relatively mismatched, with return loss values mostly above -10 dB across the entire frequency range. While the qualitative trends across all three antenna configurations match well with the reference, the depth and exact location of resonances show slight discrepancies, which may be attributed to differences in substrate parameters, simulation settings, or geometric precision during reconstruction. Nonetheless, the results validate the general behavior and design trends described in the original study.

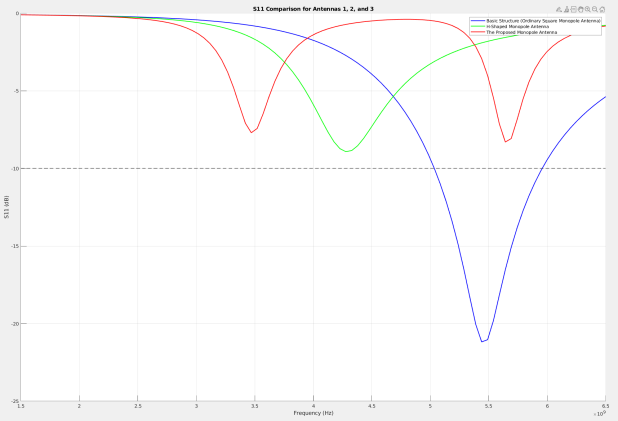

Fig. 8: Simulated reflection coefficients S_{11}

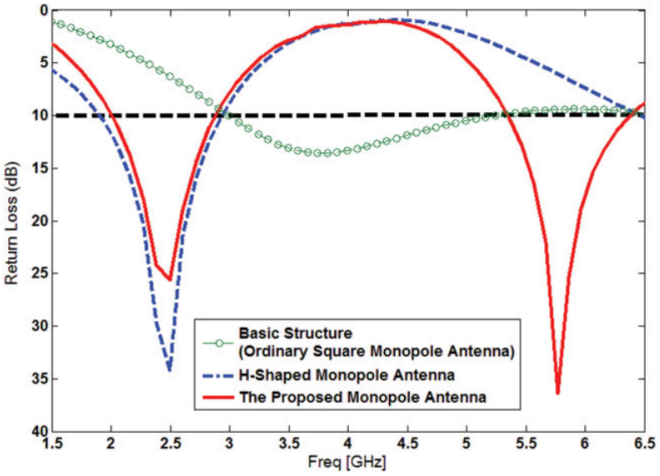

Fig. 9: Simulated reflection coefficients S_{11} (Paper results)

B. Radiation Characteristics

At 2.4 GHz and 5.8 GHz (Figure 11), the paper's antenna demonstrates a relatively directional co-polarization (co-pol) response in both the E-plane (y-z plane) and H-plane (x-z plane), with minimal cross-polarization (cross-pol), indicating strong polarization. In the reconstructed patterns at 3.4 GHz and 5.6 GHz (Figure 10), a similar directional co-pol behavior is observed. The co-pol lobes exhibit the expected figure-eight shapes in the E-plane and more omnidirectional characteristics in the H-plane, consistent with the original results. The cross-pol levels in the reconstructed results remain significantly lower than the co-pol levels, as in the original, though slightly higher side-lobe levels and asymmetries can be noted, particularly in the H-plane plots. These discrepancies again, may arise from variations in simulation conditions, feed location and diameter or measurement setup.

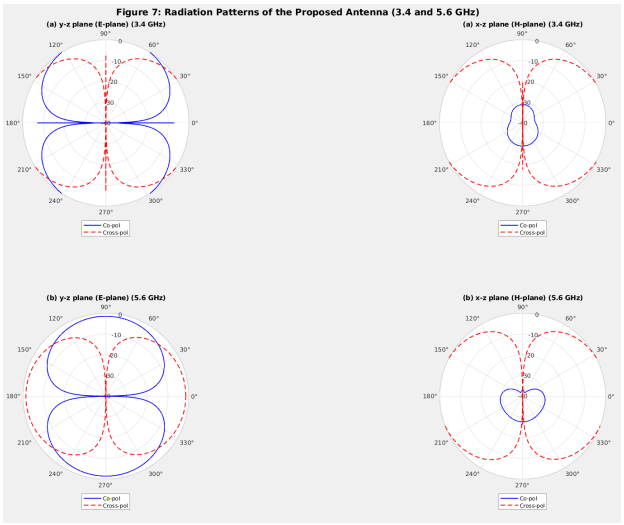

Fig. 10: Radiation Patterns for the proposed antenna at 3.4 and 5.6 GHz

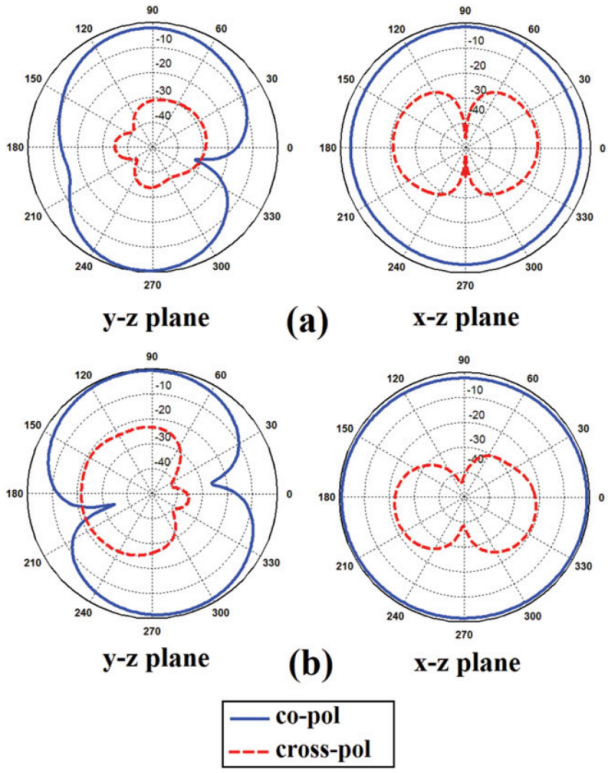

Fig. 11: Radiation Patterns for the proposed antenna at 2.4 and 5.8 GHz (Paper results)

C. Gain Performance

The gain characteristics, shown in Figure 12, demonstrate the antenna's dual-band operation:

For the 2.4 GHz band (subplot (a)), the original paper reports a peak gain of approximately 2.9 dBi at 2.4 GHz, with the gain steadily decreasing outside this frequency. In contrast, our reconstructed results show a lower peak gain of around 1.2 dBi near 3.3 GHz, with a noticeable frequency shift and reduced performance across the desired 2.4 GHz band.

Similarly, for the 5.8 GHz band (subplot (b)), the reference design exhibits a peak gain of about 4.2 dBi at 5.8 GHz. However, our implementation yields a peak gain of only around 1.6 dBi near the same frequency, with significantly lower gain and even negative values in the lower frequency range starting around 4.5 GHz. These discrepancies again, may stem from differences in simulation environment, feed location and diameter, mesh fabrication etc.

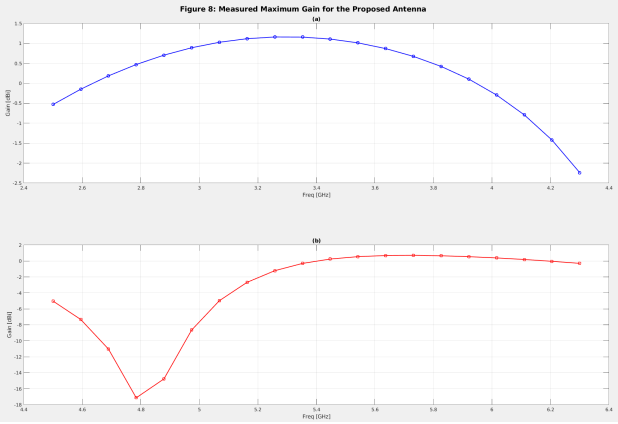

Fig. 12: Gain Performance of the proposed antenna

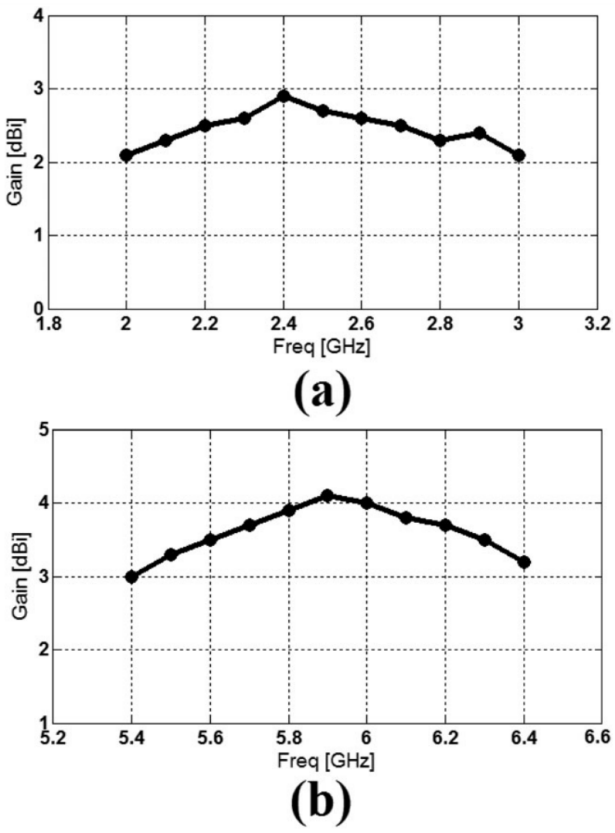

Fig. 13: Gain Performance of the proposed antenna (Paper results)

D. Smith Charts

The Smith chart results from the proposed antenna in the paper (Figure 15) and the simulated input impedance from my analysis are compared to evaluate the performance of the antenna design. The Smith chart in the paper displays the impedance characteristics of the antenna, likely indicating a well-matched impedance near the center of the chart, which suggests efficient power transfer and minimal reflection.

In contrast, the simulated results from my design (Figure 14) show impedance points distributed across the chart, including regions with significant reactance components (e.g., $+j1$, $+j3$, $-j5$). This indicates potential mismatches or resonant behavior at certain frequencies, which may require further tuning to achieve optimal performance. While the paper's results demonstrate a refined design, the discrepancies in this work highlight areas for improvement, such as adjusting the antenna geometry or feed configuration to better align with the desired impedance matching.

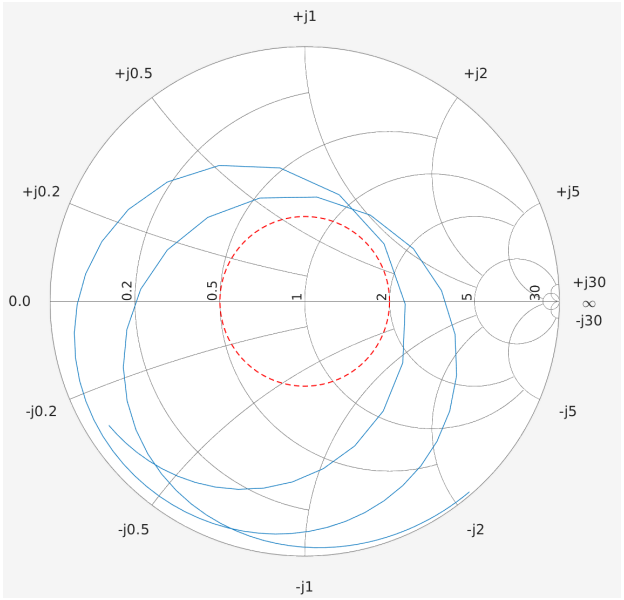

Fig. 14: Simulated input impedance on a smith chat for the proposed antenna

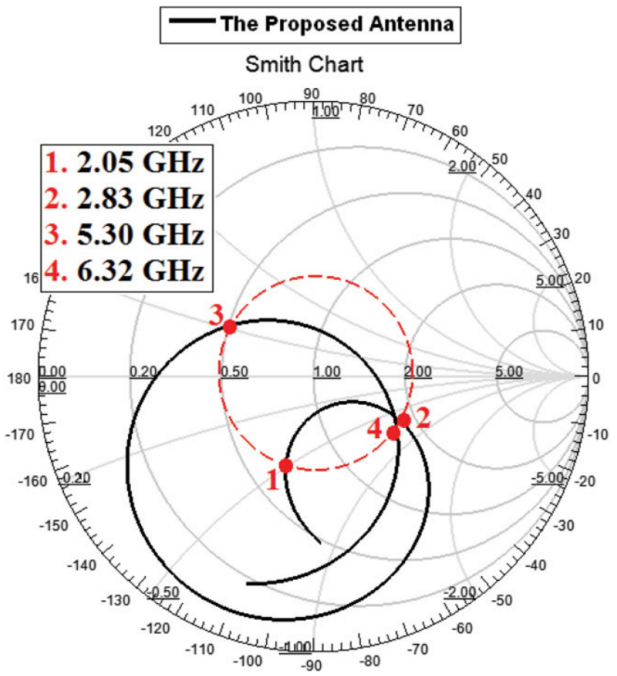

Fig. 15: Simulated input impedance on a smith chat for the proposed antenna (Paper results)

E. Current Distributions

The current distribution patterns from the reference paper (Figure 19) and my analysis (Figures 16, 17 and 18) reveal important insights about antenna performance. The reference results show optimized current flow at both 2.4 GHz and 5.8 GHz for their proposed design, with particularly strong currents along the radiating edges at the higher frequency.

My simulations demonstrate comparable current concentrations at similar frequencies (3.4 GHz and 5.6 GHz), though with some spatial variations in current density. The H-shaped antenna results (Figure 16) at 4.3 GHz show current localization patterns that differ from both the reference design and our proposed antenna, particularly in the y-axis distribution (maximum 0.005 m versus 0.004 m in our design). The 5.6 GHz results exhibit stronger current magnitudes along the x-axis (peaking at 0.025 m) compared to the reference 5.8 GHz data, suggesting possible frequency-dependent behavior or geometric optimization opportunities.

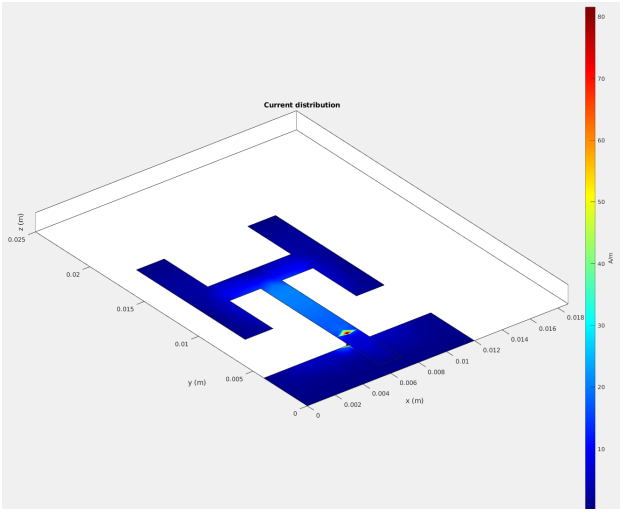

Fig. 16: Current Distribution for the H shaped antenna at 4.3 GHz

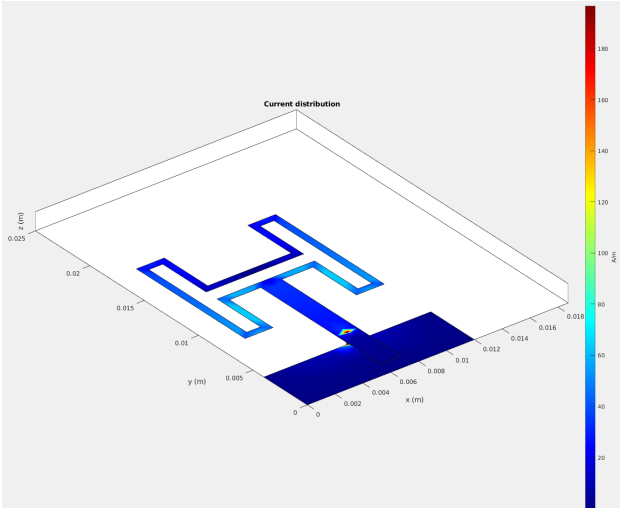

Fig. 17: Current Distribution for the proposed antenna at 3.4 GHz

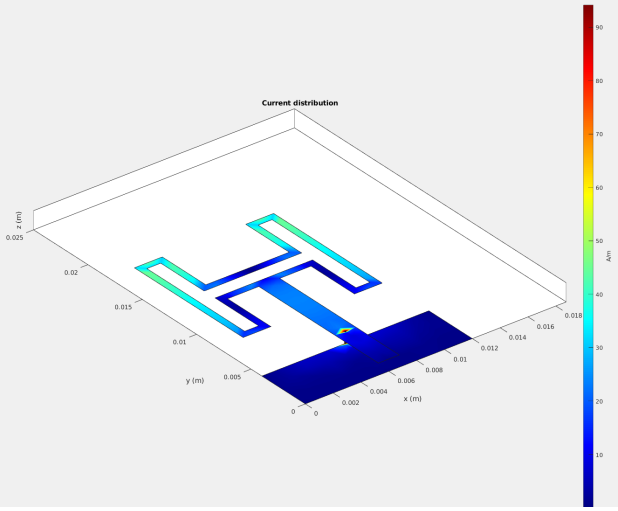

Fig. 18: Current Distribution for the proposed antenna at 5.6 GHz

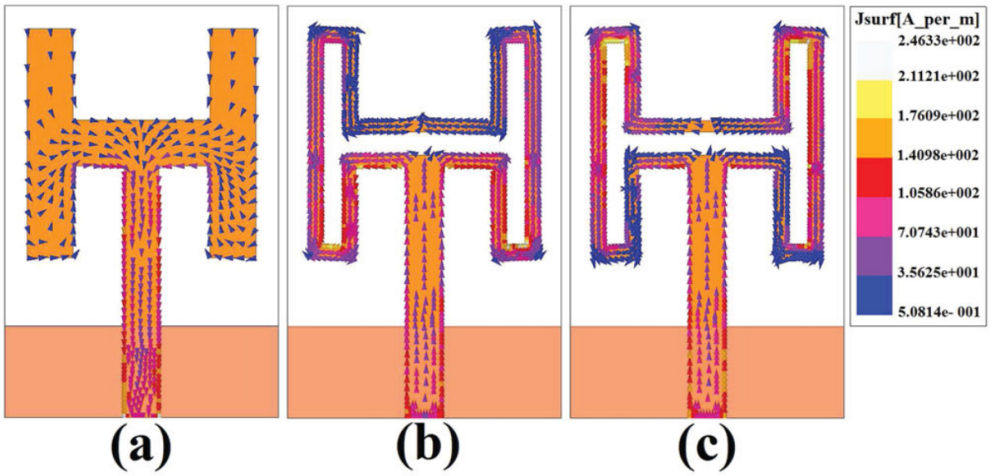

Fig. 19: Current Distribution for the proposed antenna (Paper results)

III. INSIGHTS

The simulation results do not fully confirm the antenna's performance as reported in the article. Minor discrepancies are observed, which can be attributed to factors such as feed location and diameter, mesh discretization settings, and assumptions regarding material parameters.

IV. CONCLUSION

Overall, the design progression from Antenna 1 to Antenna 3 showcases a systematic enhancement in performance through geometric optimization and resonant mode manipulation, guided by electromagnetic simulation and impedance matching principles.

The MATLAB Antenna Toolbox proves to be a powerful tool for replicating complex antenna designs. Through this assignment, valuable insights were gained on both antenna modeling and electromagnetic simulation.

V. POSTSCRIPT

I tried placing the feed at the edge of the ground plane, at $(x, y) = \left(\frac{W_{\text{sub}}}{2}, 0\right)$, and also tested different feed diameters. However, all of these attempts resulted in noticeably worse performance compared to what is reported in my paper.